

# Searching for near-horizon quantum structures in the binary black-hole stochastic gravitational-wave background

Song Ming Du<sup>1,\*</sup> and Yanbei Chen<sup>1</sup>

<sup>1</sup>*Theoretical Astrophysics and Walter Burke Institute for Theoretical Physics,  
California Institute of Technology, Pasadena, California 91125, USA*

(Dated: March 30, 2018)

It has been speculated that quantum gravity corrections may lead to modifications to space-time geometry near black hole horizons. Such structures may cause reflections to gravitational waves, causing *echoes* that follow the main gravitational waves from binary black hole coalescence. We show that such echoes, if exist, will give rise to a stochastic gravitational-wave background, which is very substantial if the near-horizon structure has a near unity reflectivity for gravitational waves, readily detectable by Advanced LIGO. In case reflectivity is much less than unity, the background will mainly be arising from the first echo, with a level proportional to the power reflectivity of the near-horizon structure, but robust against uncertainties in the location of the structure — as long as it is very close to the horizon. Sensitivity of third-generation detectors allows the detection of a background that corresponds to power reflectivity  $\sim 10^{-3}$ , if the uncertainties in the binary black-hole merger rate can be removed. We note that the echoes do alter the  $f^{2/3}$  power law of the background spectra at low frequencies, which is rather robust against the uncertainties.

PACS numbers:

*Introduction.*— Black holes (BH) are monumental predictions of general relativity (GR) [1]. It is often believed that, inside a black hole, a singularity exists, around which general relativity, a classical description of space-time geometry will break down, and needs to be replaced by a full quantum theory of gravity (QTG). The Planck scale of  $l_p \sim 1.6 \times 10^{-35}$  m is often cited as the scale at which full-blown QTG is required. However, interesting effects already arise as one applies quantum mechanics to fluctuations around the black-hole’s horizon, the boundary of the region from which one can escape toward infinity — even though space-time curvature does not blow up near the horizon. Hawking showed that black holes evaporate — which consequently lead to the so-called Black-Hole Information Paradox. During attempts to resolve this Paradox — as well as in other contexts — it was proposed that space-time geometry near the horizon may differ from the Kerr geometry, by having additional, quantum structures [2]. Candidate proposals include firewall [3], fuzzball [4] and gravastar [5].

Detection of gravitational waves (GW) generated by binary black-hole (BBH) collisions marked the dawn of GW astronomy [6], and brings us an experimental tool to study the physical nature of BH horizon. A recent study [7, 8] suggested that the three GW events (GW150914, GW151226 and LVT151012) provide positive evidence towards the existence of Planck scale structures near the horizon by finding *echoes* of GWs, reflected from these structures — although it has not been resolved whether such echoes were really detected with sufficient statistical significance [9]. Furthermore, the particular echo model employed by [7, 8] was considered rather naive and needed refinement [10]. For example, Mark *et al.*, using scalar field generated by a point particle falling into a Schwarzschild black hole, illustrated that, the echoes can have a variety of time-domain features, which depend on the location, and (in general frequency-dependent) reflectivity of the near-horizon structure [11].

In this letter, we propose to search for near-horizon structures via the stochastic gravitational-wave background (SGWB) from binary black-hole mergers. Because the echo contribution to the background depends only on their energy spectra, it is much less sensitive to details of echo generation, therefore making the method more robust to uncertainties in the near-horizon structures. We estimate the magnitude and rough feature of the additional background — and illustrate its dependence on the near-horizon structure — following an Effective One-Body (EOB) approach. In this approach the two-body dynamics and waveform is approximated by the plunge of a point particle toward a Schwarzschild black hole, following a trajectory that smoothly transitions from inspiral to plunge [12, 13].

*GW amplitudes and power emitted.*— GWs emitted from a test particle plunging into a Schwarzschild BH can be described by the Sasaki-Nakamura (SN) equation [14]:

$$\left(\partial_{r_*}^2 + \omega^2 - V_l(r)\right)X_{lm}(\omega, r_*) = S_{lm}(\omega, r), \quad (1)$$

where  $r_*$  is the tortoise coordinate with  $dr/dr_* = 1 - 2M/r$  with effective potential given by

$$V_l(r) = \left(1 - \frac{2M}{r}\right) \left(\frac{l(l+1)}{r^2} - \frac{6M}{r^3}\right). \quad (2)$$

with  $M$  the mass of the black hole. The source term is given by  $S_{lm}(\omega, r) = W_{lm}(\omega, r)r^{-5}e^{-i\omega r_*}$ , where  $W_{lm}$  is a functional of the trajectory of the test particle and its explicit expression can be found in Eqs. (19)–(21) of [14]. The wave function  $X_{lm}$  is related to GW in the  $r \rightarrow +\infty$  limit via  $h_+ + ih_\times = 8r^{-1} \sum_{lm} {}_{-2}Y_{lm}X_{lm}(t)$ , where  ${}_sY_{lm}$  are spin- $s$  weighted spherical harmonics and  $X_{lm}(t) = \int_{-\infty}^{+\infty} d\omega e^{-i\omega t}X_{lm}(\omega)$ . The GW energy spectrum is given by

$$dE/d\omega = \sum_{lm} 16\pi\omega^2 |X_{lm}(\omega, r_* \rightarrow \infty)|^2. \quad (3)$$

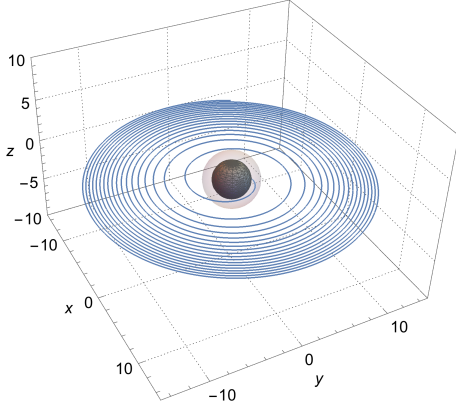


FIG. 1: The trajectory of the EOB effective particle moving in a coalescing quasi-circular orbit. The symmetric mass ratio  $\nu = 0.25$ . The inner black sphere with radius  $r = 2M$  represents the event horizon of a Schwarzschild BH. The outer translucent sphere with radius  $r = 3M$  represents the light ring.

For black holes, imposing in-going boundary condition near the horizon and out-going condition near null infinity, solution to Eq. (1) is expressed as  $X_{lm}^{(0)}(\omega, r_* \rightarrow \infty) = e^{i\omega r_*} Z_{lm}^{(0)}(\omega)$ , with

$$Z_{lm}^{(0)}(\omega) = \int_{-\infty}^{+\infty} dr'_* \frac{S_{lm}(\omega, r'_*) X_{in}^{(0)}(\omega, r'_*)}{W^{(0)}(\omega)}, \quad (4)$$

with  $W^{(0)} = X_{in}^{(0)} \partial_{r_*} X_{out}^{(0)} - X_{out}^{(0)} \partial_{r_*} X_{in}^{(0)}$  the Wronskian between the two homogenous solutions defined with boundary conditions  $X_{in}^{(0)} \sim e^{-i\omega r_*}$  for  $r_* \rightarrow -\infty$  and  $X_{out}^{(0)} \sim e^{+i\omega r_*}$  for  $r_* \rightarrow +\infty$  respectively.

*Echoes from near-horizon structure.*— Suppose a correction to Schwarzschild geometry takes place very close to the horizon, creating an *additional potential barrier*  $V_p$ . We have  $V_l \rightarrow V_l + V_p$ , with  $V_p$  centered at  $r^p = 2M + \epsilon$ . Here  $\epsilon$  is a small distance related to  $l_p$ . In tortoise coordinate,  $\epsilon = l_p$  corresponds to  $r_*^p \approx -182M$ .

As discussed by [11] the influence from  $V_p$  can be described by replacing the horizon ( $r_* \rightarrow -\infty$ ) boundary condition for Eq. (1) into

$$X_{in}^{(R)} \sim e^{-i\omega r_*} + \mathcal{R} e^{i\omega r_*} \quad \text{for } r_* \rightarrow r_*^p, \quad (5)$$

while keeping the  $r_* \rightarrow +\infty$  boundary condition unchanged. Here,  $\mathcal{R}(\omega)$  can be viewed as a (complex) reflectivity of the potential barrier.

Equation (5) does not explicitly contain the location of reflection, which is implicitly contained in the frequency dependence of  $\mathcal{R}(\omega)$ . For example, a Dirichlet boundary condition corresponds to  $\mathcal{R}_D = -e^{2i\omega r_*^p}$ . In general, if  $\mathcal{R}(\omega) = \rho(\omega) e^{i\psi(\omega)}$  with  $\rho(\omega)$  a slowly varying complex amplitude and  $\psi$  a fast-varying phase, then the effective location of reflection for a wavepacket with central frequency  $\omega_0$  is around  $[\partial\psi/\partial\omega]_{\omega=\omega_0}/2$ .

As discussed in [11], the result  $X_{lm}^{(R)} = Z_{lm}^{(R)} e^{i\omega r_*}$  can be expressed by the original homogenous solutions:

$$Z_{lm}^{(R)} = (Z_{lm}^{(0)} + \mathcal{R} \bar{Z}_{lm}^{(0)}) / (1 - \mathcal{R} \mathcal{R}_{BH}), \quad (6)$$

where  $Z_{lm}^{(0)}$  is defined in Eq. (4),  $\mathcal{R}_{BH}$  is the complex reflectivity of the Regge-Wheeler potential  $V_l$ , which is defined by Eq. (2.14) of [11], and  $\bar{Z}_{lm}$  is

$$\bar{Z}_{lm}^{(0)}(\omega) = \int_{-\infty}^{+\infty} dr'_* \frac{S_{lm}(\omega, r'_*) \bar{X}_{in}^{(0)}(\omega, r'_*)}{W^{(0)}(\omega)}, \quad (7)$$

with  $\bar{X}_{in}^{(0)}$  the complex conjugate of  $X_{in}^{(0)}$

As we expand the above expression in  $\mathcal{R}$ , we write the outgoing wave in a series of echoes:

$$Z_{lm}^{(R)} = Z_{lm}^{(0)} + \mathcal{R} \underbrace{(\bar{Z}_{lm}^{(0)} + \mathcal{R}_{BH} Z_{lm}^{(0)})}_{Z_{lm}^{(1)}} \sum_{n=0}^{+\infty} (\mathcal{R} \mathcal{R}_{BH})^n. \quad (8)$$

The summation is over echoes, each delayed from the earlier one by  $\sim 2|r_*^p|$ . In case of small  $\mathcal{R}$ , we write  $Z_{lm}^{(R)} \approx Z_{lm}^{(0)} + \mathcal{R} Z_{lm}^{(1)}$  and

$$(dE/d\omega)_R \approx 16\pi\omega^2 \sum_{lm} |Z_{lm}^{(0)} + \mathcal{R} Z_{lm}^{(1)}|^2. \quad (9)$$

*A Model of Reflectivity and Energy Spectrum of Echoes.*—

One can assume physically that the reflectivity is small for high frequencies and approaches to unity for low frequencies, e.g.,

$$\mathcal{R}(\omega) = e^{2i\omega r_*^p} \mathcal{A} / (2i\omega - \mathcal{A}), \quad (10)$$

with  $\mathcal{A}$  a constant. This corresponds to an effective potential  $V_p = \mathcal{A} \delta(r_* - r_*^p)$ . This  $\delta$ -function potential can be used to approximate narrow potentials with area  $\int_{-\infty}^{+\infty} dr_* V_p(r_*) = \mathcal{A}$ . Note that  $M\mathcal{A}$  is a dimensionless quantity. As a comparison, the area under the Regge-Wheeler potential is [15]  $M \int V_l dr_* = (l-1)(l+2)/2 + 1/4$ .

To make a first estimate of the energy spectrum due to echos, we adopt the *leading* EOB approximation [12, 13]: for black holes with  $m_1$  and  $m_2$ , we consider a point particle with reduced mass  $\mu = m_1 m_2 / (m_1 + m_2)^2$  falling down a

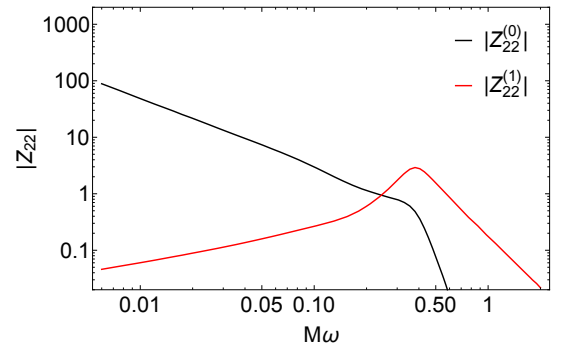


FIG. 2: The main wave  $Z_{22}^{(0)}$  and the wave  $Z_{22}^{(1)}$  that generates echoes.

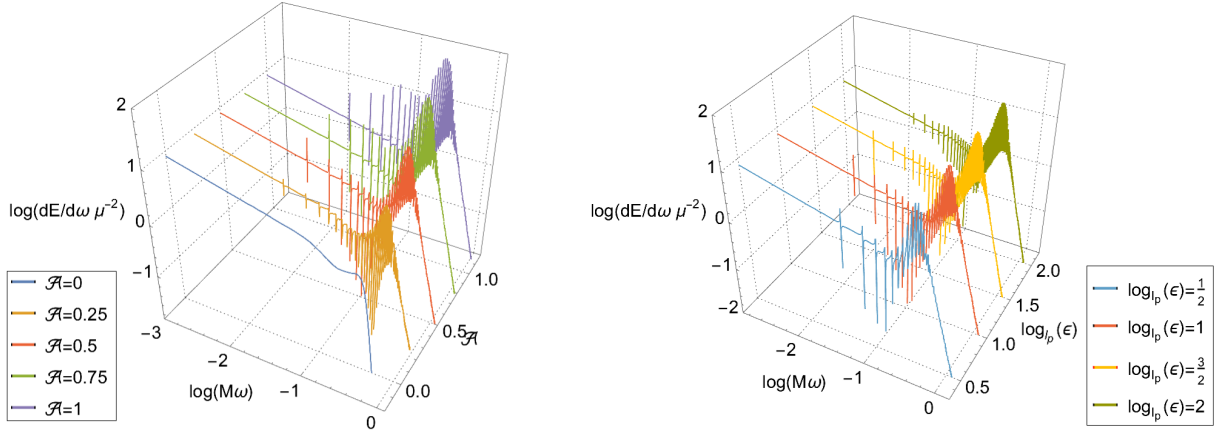


FIG. 3: Left Panel: The energy spectra of GW emission from  $\nu = 0.25$  coalescing BBH for different values of  $M\mathcal{A}$ . The correction  $V_p$  corresponds to Eq. (10) with  $\epsilon = l_p$ . Right Panel: The energy spectra of GW emission from  $\nu = 0.25$  coalescing BBH for  $M\mathcal{A} = 0.5$  with different values of  $\epsilon$ .

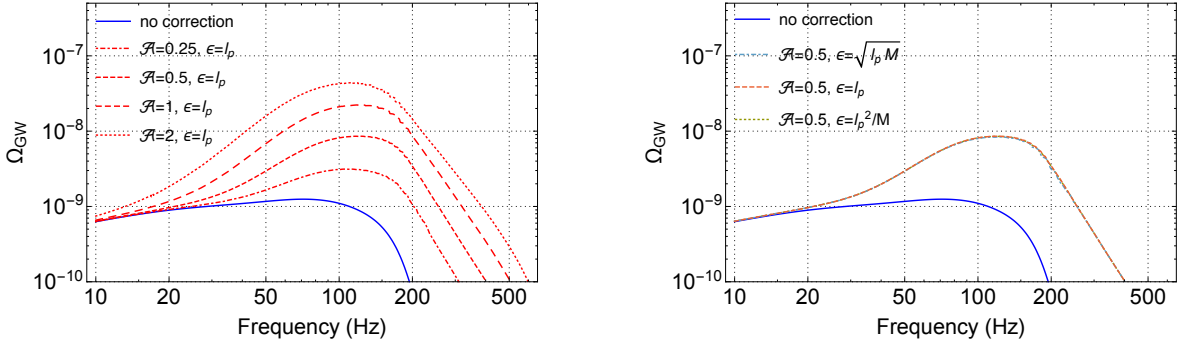


FIG. 4: Left panel: The spectral energy density  $\Omega_{\text{GW}}(f)$  with different values of area under correction  $V_p$ . Right panel: The spectral energy density  $\Omega_{\text{GW}}(f)$  with the varied locations of correction  $V_p$  while the area keeps constant.

Schwarzschild black hole with total mass  $M = m_1 + m_2$ ; the symmetric mass ratio is defined as  $\nu = \mu/M$ .

For motion in the equatorial plane, we have a Hamiltonian for  $(r, p_r, \phi, p_\phi)$ , with radiation reaction force added as a generalized force  $\mathcal{F}_\phi$  [Eqs. (3.41)–(3.44) of [13]]. For  $\nu = 0.25$ , we plot the trajectory in Fig. 1. Upon obtaining the time-domain trajectory, we obtain source term  $S_{lm}$ , and compute  $Z_{lm}$  and  $\bar{Z}_{lm}$  according to Eqs. 4 and 7, which will then lead to the energy spectrum of the emitted gravitational waves.

Since for coalescing BBH, most of the energy emitted from GW is from  $(l, m) = (2, 2)$ , from now on we only consider the  $(2, 2)$  mode in the study of energy spectrum and SGWB. As can be seen in Fig. 2, the main wave  $|Z_{22}^{(0)}|$  recovers the  $f^{-7/6}$  power law at low frequencies, as predicted by post-Newtonian approximation, also qualitatively mimics a BBH waveform at intermediate to high frequencies. The wave  $|Z_{22}^{(1)}|$  peaks roughly at the quasi-normal mode (QNM) frequency of the Schwarzschild black hole.

Horizon structures with  $M\mathcal{A}$  of order unity lead to significant modifications in GW energy spectrum  $dE/d\omega$ . In the left panel of Fig. 3, we choose  $\epsilon = l_p$  and  $M\mathcal{A} = 0.25, 0.5, 0.75$  and 1. At low frequencies, the near-horizon struc-

tures add peaks separated by  $\Delta\omega \sim 0.017M^{-1} \sim \pi/r_*^p$  to the  $dE/df \propto f^{-1/3}$  power law, as predicted by post-Newtonian approximation. Near the QNM frequency, there is substantial additional radiation. In the right panel, we choose several different values of  $\epsilon$  which lead to different peak separation at low frequencies. For small values of  $\mathcal{A}$ , in the main detection band, we can approximate

$$\left(\frac{dE}{d\omega}\right)_R = 16\pi\omega^2 \left[ |Z_{22}^{(0)}|^2 + \frac{\mathcal{A}^2 |Z_{22}^{(1)}|^2}{4\omega^2} - \frac{\mathcal{A} \text{Im}(Z_{22}^{(0)} \bar{Z}_{22}^{(1)} e^{-2i\omega r_*^p})}{\omega} \right]. \quad (11)$$

with  $\bar{Z}_{22}^{(1)}$  the complex conjugate of  $Z_{22}^{(1)}$ , as a sum of energies from *main wave*, the *first echo*, and the *beat* between the main wave and the first echo. While the beat is linear in  $\mathcal{A}$ , it is highly oscillatory in the frequency domain, since the main wave and the echo are well separated in the time domain. As we shall see below, for negative enough  $r_*^p$ , the beat term, this oscillation tends to cancel out between different sources, suppressing the effect of the beating term in the stochastic background.

*Stochastic Gravitational-Wave Background (SGWB).*– The

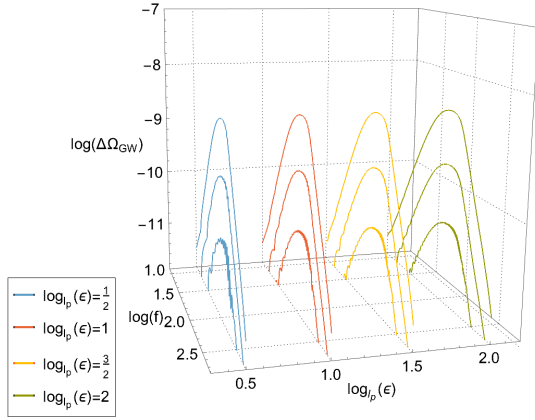


FIG. 5:  $\Delta\Omega_{\text{GW}}$  as functions of  $f$ , for for  $\mathcal{A} = 0.3, 0.1$  and  $0.03$ , and  $\epsilon/M = (l_p/M)^{1/2, 1.3/2.2}$ . Here  $\Delta\Omega$  mainly scales with  $\mathcal{A}^2$ , except the oscillations shown for small values of  $\mathcal{A}$  and large values of  $\epsilon$ , in which case oscillations in the beating term of Eq. (11) did not completely get smoothed out.

SGWB is usually expressed as

$$\Omega(f) = \rho_c^{-1} d\rho_{\text{GW}}/d \ln f, \quad (12)$$

where  $\rho_c$  represents the critical density to close the universe and  $\rho_{\text{GW}}$  the GW energy density; it is related the  $dE/df$  of a single GW source via [16]

$$\Omega(f) = \frac{f}{\rho_c} \int_0^{z_{\text{max}}} dz \frac{R_m(z)[dE/df]_{f_z}}{(1+z)H(z)}, \quad (13)$$

where  $f_z = f(1+z)$  is the frequency at emission. Here we adopt the  $\Lambda$ CDM cosmological model with  $H(z) = H_0[\Omega_M(1+z)^3 + \Omega_\Lambda]^{1/2}$ , where the Hubble constant  $H_0 = 70\text{km/s Mpc}$ ,  $\Omega_M = 0.3$  and  $\Omega_\Lambda = 0.7$ .  $R_m(z)$  is the BBH merger rate per comoving volume at redshift  $z$ . We use the Fiducial model described in [17], where  $R_m(z)$  is proportional to the star formation rate with metallicity  $Z < Z_\odot/2$  and delayed by the time between BBH formation and merger. As in the Fiducial model, the parameters of BBH follow GW150914:  $M = 65M_\odot$ ,  $\nu = 0.25$  with a local merger rate  $R_m(0) = 16\text{Gpc}^{-3} \text{yr}^{-1}$ .

For  $M\mathcal{A} \sim 1$ , we get substantial additional SGWB from the echoes, as shown in Fig. 4 (left panel), in a way that is insensitive to the location of the near-horizon structure,  $\epsilon$  (right panel). For lower values of  $M\mathcal{A}$ , we plot the *additional* background, defined as  $\Delta\Omega \equiv \Omega_{\mathcal{A}>0} - \Omega_{\mathcal{A}=0}$  in Fig. 5, for different values of  $\mathcal{A}$  and  $\epsilon$ . Here  $\Delta\Omega$  is mainly proportional to  $\mathcal{A}^2$ , values of  $\mathcal{A} > 0.03$  and  $\epsilon/M < \sqrt{l_p M}$ : the beating between the main wave and the echoes are not important, and the background mainly arise from energy contained in the first echo.

*Detectability.*— The optimal signal-to-noise ratio (SNR) for a SGWB between a pair of detectors is given by  $\sqrt{\langle\Omega|\Omega\rangle}$  [18], with

$$\langle\Omega_A|\Omega_B\rangle \equiv 2T \left( \frac{3H_0^2}{10\pi^2} \right)^2 \int_0^{+\infty} df \frac{\Omega_A(f)\gamma^2(f)\Omega_B(f)}{f^6 P_1(f)P_2(f)}, \quad (14)$$

where  $\gamma(f)$  is the normalized overlap reduction function between the detectors, and  $P_{1,2}(f)$  are the detectors' noise spectral densities. We consider advanced LIGO at design sensitivity [19], LIGO Voyager [20] and Einstein Telescope (ET) [21] at planned sensitivities. Advanced LIGO and LIGO Voyager have the same  $\gamma$  and we take the constant  $\gamma = -3/8$  for co-located ET detectors [22]. The 1-year SNRs are listed in Table I for values of  $M\mathcal{A}$  at order unity, in which case the echoes contribute significantly to the SNRs.

$\mathcal{A}$	LIGO	Voyager	ET
0	1.42	27.5	196
0.5	2.15	40.9	513
1	3.99	75.2	1215
2	8.76	164.7	2561

TABLE I: One-year SNR of three generations of GW detectors for SGWB  $\Omega_{\mathcal{A}}$  with different values of  $\mathcal{A}$ .

For lower values of  $\mathcal{A}$ , in order to distinguish the SGWB with and without contribution from the echoes, we apply the model-selection method described in [18]. The log-likelihood ratio between two models is given by

$$\ln \Lambda = \langle\Delta\Omega|\Delta\Omega\rangle/4, \quad (15)$$

with two models considered discernible when  $\ln \Lambda > 3$ . In Table II, we show the minimal distinguishable  $M\mathcal{A}$  to reach this log-likelihood ratio threshold. In particular, with 5-year integration, Voyager can detect  $M\mathcal{A} \approx 0.15$ , while ET can detect  $M\mathcal{A} \approx 0.028$ .

$T$	LIGO	Voyager	ET
1 yr	1.15	0.22	0.043
5 yrs	0.70	0.15	0.028

TABLE II: The minimal distinguishable  $M\mathcal{A}$  to reach a log-likelihood ratio  $\ln \Lambda > 3$  for three generations of GW detector with different integration times.

*Conclusions and Discussions.*— As we have seen in this paper, the  $\Delta\Omega$  due to the echoes is largely independent from uncertainties in  $r_*^p$ . For strong near-horizon structures, with  $\mathcal{A}$  the order of unity, the additional background from the echoes will be clearly visible. For weak near-horizon structures,  $\Delta\Omega$  is mainly given by the first echo, and is simply proportional to the power reflectivity  $|\mathcal{R}|^2$ . The level detectable by ET roughly corresponds to  $M\mathcal{A} \sim 0.028$ , which corresponds to  $|\mathcal{R}|^2 \approx 10^{-3}$  near the peak of the echo energy spectrum. Further details of the background not only depends on details in the additional potential barrier  $V_p$ , we will also need to generalize the analysis to a Kerr background.

We should also be aware of uncertainties in the SGWB of the main, inspiral-merger-ringdown wave, e.g., arising from different star formation rates, different metallicity thresholds to form black holes, details in the evolution of binary stars and the distributions in the time delay between BBH formation and merger, — all of these lead to uncertainties in the

local BBH merger rate and the local distribution of mass  $M$  and symmetric mass ratio  $\nu$  [17]. It is believed these uncertainties can be well quantified and will be narrowed down by future BBH detections. For example, the range of BBH local merger rate has been narrowed down to  $12 - 213 \text{ Gpc}^{-3} \text{ yr}^{-1}$  after the detection of GW170104 [23]. On the other hand, as demonstrated by Zhu *et al.*, these uncertainties only scale the background spectra linearly at low frequencies and hence keep the power law  $\Omega(f) \propto f^{2/3}$  for  $f < 100 \text{ Hz}$  unchanged [16]. Our result shows the appearance of the near-horizon structures changes the slope and the  $f^{2/3}$  power law is deviated even at low frequencies. This fact should be included in further analysis to alleviate the influence from uncertainties.

*Acknowledgements.*— This work is supported by NSF Grants PHY-1708212 and PHY-1404569 and PHY-1708213. and the Brinson Foundation. We thank Yiqiu Ma, Zachary Mark, Aaron Zimmerman for discussions, in particular ZM and AZ for sharing insights on the echoes. We are grateful to Eric Thrane and Xing-Jiang Zhu for providing feedback on the manuscript.

---

\* Electronic address: smdu@caltech.edu

- [1] V. Frolov and I. Novikov, *Black hole physics: basic concepts and new developments*, vol. 96 (Springer Science & Business Media, 2012).
- [2] S. B. Giddings, *Classical and Quantum Gravity* **33**, 235010 (2016).
- [3] A. Almheiri, D. Marolf, J. Polchinski, and J. Sully, *Journal of High Energy Physics* **2013**, 62 (2013).
- [4] S. D. Mathur, *Fortschritte der Physik* **53**, 793 (2005).
- [5] P. O. Mazur and E. Mottola, arXiv preprint gr-qc/0109035 (2001).
- [6] B. P. Abbott, R. Abbott, T. Abbott, M. Abernathy, F. Acernese, K. Ackley, C. Adams, T. Adams, P. Addesso, R. Adhikari, et al., *Physical review letters* **116**, 061102 (2016).
- [7] J. Abedi, H. Dykaar, and N. Afshordi, arXiv preprint arXiv:1612.00266 (2016).
- [8] J. Abedi, H. Dykaar, and N. Afshordi, arXiv preprint arXiv:1701.03485 (2017).
- [9] G. Ashton, O. Birnholtz, M. Cabero, C. Capano, T. Dent, B. Krishnan, G. D. Meadors, A. B. Nielsen, A. Nitz, and J. Westerweck, arXiv preprint arXiv:1612.05625 (2016).
- [10] R. Price and G. Khanna, arXiv preprint arXiv:1702.04833 (2017).
- [11] Z. Mark, A. Zimmerman, S. M. Du, and Y. Chen, *Physical Review D* **96**, 084002 (2017).
- [12] A. Buonanno and T. Damour, *Physical Review D* **59**, 084006 (1999).
- [13] A. Buonanno and T. Damour, *Physical Review D* **62**, 064015 (2000).
- [14] M. Sasaki and T. Nakamura, *Physics Letters A* **87**, 85 (1981).
- [15] S. Chandrasekhar and S. Detweiler, *Proceedings of the Royal Society of London. Series A, Mathematical and Physical Sciences* pp. 441–452 (1975).
- [16] X.-J. Zhu, E. J. Howell, D. G. Blair, and Z.-H. Zhu, *Monthly Notices of the Royal Astronomical Society* **431**, 882 (2013).
- [17] B. Abbott, R. Abbott, T. Abbott, M. Abernathy, F. Acernese, K. Ackley, C. Adams, T. Adams, P. Addesso, R. Adhikari, et al., *Physical review letters* **116**, 131102 (2016).
- [18] T. Callister, L. Sammut, S. Qiu, I. Mandel, and E. Thrane, *Physical Review X* **6**, 031018 (2016).
- [19] P. Ajith, *Physical Review D* **84**, 084037 (2011).
- [20] LIGO Document T1400316 (2015).
- [21] B. S. Sathyaprakash and B. F. Schutz, *Living Reviews in Relativity* **12**, 2 (2009).
- [22] A. Nishizawa, A. Taruya, K. Hayama, S. Kawamura, and M.-a. Sakagami, *Physical Review D* **79**, 082002 (2009).
- [23] B. Abbott, R. Abbott, T. Abbott, F. Acernese, K. Ackley, C. Adams, T. Adams, P. Addesso, R. Adhikari, et al., *Physical Review Letters* **118**, 221101 (2017).